Report 2014 - 03
March

History of Cavity Beam Position Monitors

Xiangcheng Chen

GSI Helmholtzzentrum für Schwerionenforschung GmbH
Planckstraße 1 · D-64291 Darmstadt · Germany
Postfach 11 05 52 · D-64220 Darmstadt · Germany

History of Cavity Beam Position Monitors

Xiangcheng Chen*

GSI Helmholtzzentrum für Schwerionenforschung, Darmstadt, Germany

February 10, 2014

In this report, we present an overview of the development history of cavity beam position monitors. The basic theory of interaction between the beam and the cavity, and beam position detection principle is formulated in the beginning. Then the different instances of cavity adopted by different accelerator facilities worldwide are described systematically. In the end, almost every reference regarding cavity beam position monitors is collected and compiled carefully in order to provide a comprehensive index and to facilitate further research in this subject.

Contents

* x.chen@gsi.de

Abbreviations

ANL	Argonne national laboratory
ATF	accelerator test facility
BINP	Budker institute of nuclear physics
BNL	Brookhaven national laboratory
BPM	beam position monitor
CBPM	cavity beam position monitor
CEA Saclay	Saclay nuclear research centre
CEBAF	continuous electron beam accelerator facility
CERN	European organization for nuclear research
CLIC	compact linear collider
CR	collector ring
CRL	Chalk River laboratories
CTF	CLIC test facility
DESY	Deutsche Elektronen-Synchrotron
ELBE	electron linac for beams with high brilliance and low emittance
ELSA	electron stretcher accelerator
Elettra	Elettra sincrotrone Trieste
EM	electromagnetic
ESA	end station A
ESR	experimental storage ring
ETA	electron test accelerator
FAIR	facility for antiproton and ion research
Fermilab	Fermi national accelerator laboratory
FFTB	final focus test beam
FLASH	free electron laser in Hamburg
FRS	fragment separator
GSI	Gesellschaft für Schwerionenforschung
HESR	high energy storage ring
HLS	Hefei light source
ILC	international linear collider
ITS	injector test stand
JLab	Thomas Jefferson national accelerator facility
JLC	Japan linear collider
KEK	high energy accelerator research organization
LCLS	linac coherent light source
LHC	large hadron collider
MAMI	Mainz microtron
NESR	new experimental storage ring
NLC	next linear collider
NML	new muon lab
R&D	research and development
RF	radio frequency
RHUL	royal Holloway, university of London
RIKEN	institute of physical and chemical research
SACLA	SPring-8 angstrom compact free electron laser
SDUVFEL	Shanghai deep ultraviolet free electron laser

SINAP	Shanghai institute of applied physics
SIS	Schwerionensynchrotron
SLAC	Stanford linear accelerator center
SPring-8	super photon ring — 8 GeV
SPS	super proton synchrotron
TESLA	TeV energy superconduction linear accelerator
TTF	TESLA test facility
TTX	Tsinghua Thomson scattering X-ray source
UCL	university college London
UNILAC	universal linear accelerator
USTC	university of science and technology of China
VLEPP	colliding linear electron-positron beams
XFEL	X-ray free electron laser

1 Introduction

The Facility for Antiproton and Ion Research (FAIR) has been proposed by the international science community more than a decade ago and started civil construction recently. This project aims at a multi-faceted forefront science program, beams of stable and unstable nuclei as well as antiprotons in a wide range of intensities and energies, with optimum beam qualities [1].

The facility (Fig.1) comprises a vital heart of superconducting double-synchrotron SIS100/300 with magnetic rigidities of 100 T m and 300 T m, respectively. After an upgrade for high intensities, the existing GSI accelerators UNILAC and SIS18 will serve as an injector. Adjacent to the large double-synchrotron is a complex set of a superconducting nuclear fragment separator (Super-FRS), an antiproton production target, cooling storage rings (CR, NESR and HESR) and experiment stations.

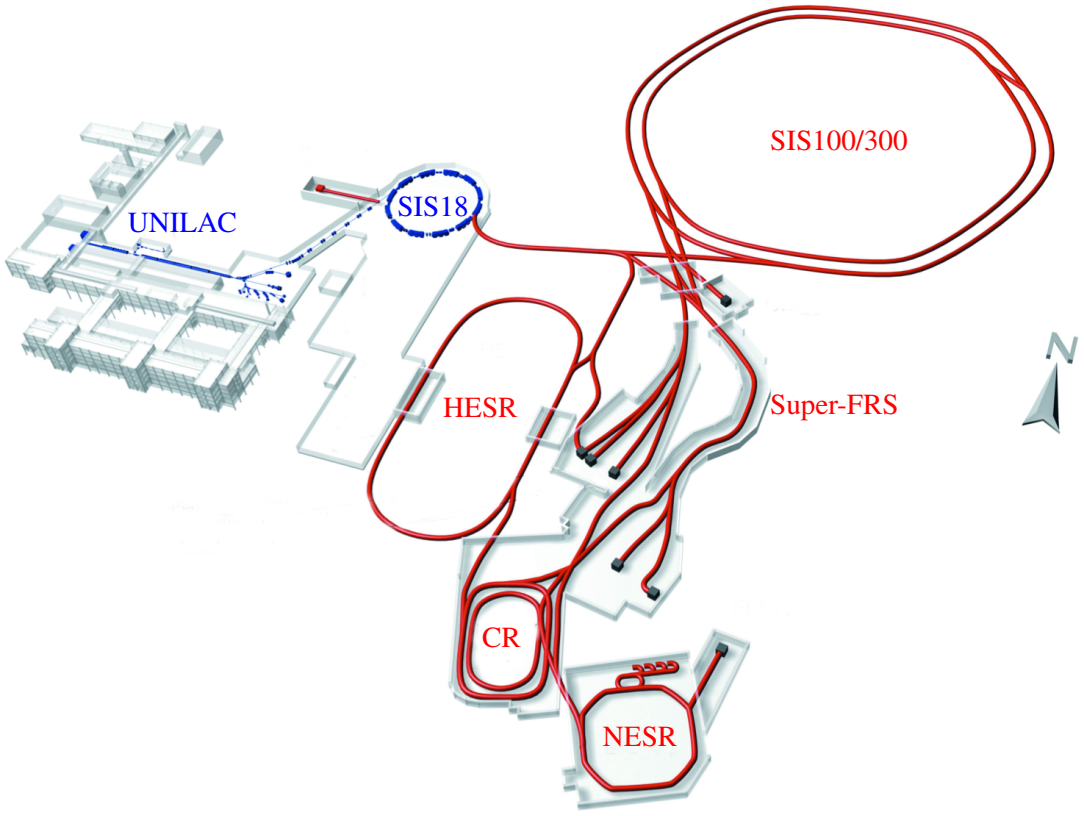

Figure 1: Layout of the existing GSI facility on the left and the planned FAIR facility on the right.

The Collector Ring (CR) is the first storage ring downstream of Super-FRS. It serves as a collector and a pre-cooler of antiprotons and radioactive ion beams for the succeeding beam lines. In order to maximize the beam transmission efficiency, a large acceptance is required as a main feature of the CR. Moreover, CR can be adopted as an isochronous mass spectrometer, which allows for high precision mass measurements of short-lived nuclides using an in-ring time-of-flight detector, when it operates in the isochronous ion-optical mode.

The isochronous mode of the CR is a sophisticated state such that stored ions of the same species but with different velocities revolve at almost the same period. The general principle is that, in simple words, a fast particle flies along an outer track in the ring while an inner track is chosen by a slow particle, which means that the lower speed is compensated by the shorter path. However due to the large acceptance of the CR, this compensation is only valid within a small range of mass-to-charge ratios which is not broad enough to cover all the injected fragments. For those ions falling out of the range, the peak widths of the revolution times will expand, thus the resolving power will deteriorate. In order to improve the resolving power of the CR, this non-isochronous effect has to be corrected for.

The measurement of magnetic rigidity of each particle could be one possible solution, as it can determine the velocity, which is sufficient to reduce the peak widths [2]. This actually means to measure the transverse position of each particle, given the fact that field strength of steering magnet is well known. As a contribution to the FAIR project, our task is to develop a position detector, in principle a beam position monitor (BPM), that is sensitive to single ions.

As important beam diagnostic devices, BPMs are widely used in many accelerators all over the world, such as linacs, cyclotrons, synchrotrons and storage rings. According to the different ways in which BPMs monitor beams, they can be generally classified as intercepting or non-intercepting. In our case, it is obvious to use non-intercepting BPMs, since the stored ions are expected to survive for a long time.

Even for non-intercepting BPMs, there also exist many types, e.g. capacitive linear-cut, button, stripline and cavity [3]. Among all these types, the cavity BPM is no doubt a promising candidate, owing to its high sensitivity of beam position and intensity detection, which we have chosen as the subject of theory investigation for the beginning phase of R&D.

It is instructive to review the previous works on cavity beam position monitors (CBPMs), in order to gain some guidelines and inspirations of designing a novel CBPM for the CR. But before that, we will first present the general theory of working principle of CBPM, which applies to various cavities.

2 Theoretical Description

The word “cavity” is derived from the Latin “cavus” (hollow) and defined as, according to the Oxford Dictionary, an empty space within a solid body. So when we talk about cavity, what we are truly interested is the shape and size of the void space rather than the enclosure body. For accelerator physicists, the word cavity, often together with radio frequency (RF), is referred to one type of components widely used in accelerators. It is usually in rectangular or circular shape and enclosed by metallic plates or chunks to confine the electromagnetic (EM) field in it.

The reason of using cavities in accelerators is to interact with charged particle beams so as to achieve different purposes: accelerating, decelerating, bunching etc. In spite of all those mentioned before which feed energy into the cavity, we can also extract energy out of it to gain the information about the beams — the way how we use a cavity as a beam current/position monitor.

In the following sections we choose a circular cavity to exemplify the theory of working principle of CBPM. The reader should note that the specific details may differ between various types of CBPM, but the general concepts will certainly apply.

2.1 Ideal Model

Let's first start with an ideal circular model, which means the hollow space is a cylinder with vacuum inside and the confining material is the perfect conductor. The EM field distribution in the empty space can be obtained by solving the Maxwell's equations. For the reason of simplicity, let's assume there are no charge sources or current sources in the cavity, and the EM field has already been established[1]. Additionally, since both relative permittivity and relative permeability of vacuum are unity, the Maxwell equations take the reduced form:

$$\nabla \cdot \boldsymbol{E} = 0\,, \tag{1a}$$
$$\nabla \cdot \boldsymbol{B} = 0\,, \tag{1b}$$
$$\nabla \times \boldsymbol{E} = -\frac{\partial \boldsymbol{B}}{\partial t}\,, \tag{1c}$$
$$\nabla \times \boldsymbol{B} = \frac{1}{c^2}\frac{\partial \boldsymbol{E}}{\partial t}\,, \tag{1d}$$

with the boundary conditions:

$$\boldsymbol{n} \times \boldsymbol{E} = 0\,, \tag{2a}$$
$$\boldsymbol{n} \cdot \boldsymbol{B} = 0\,, \tag{2b}$$

where c is the speed of light in vacuum, and $\boldsymbol{n}$ is the normal vector of the boundary.

Then we take the curl of both sides of Eq. (1c), followed by using the identity:

$$\nabla \times \nabla \times \boldsymbol{A} \equiv \nabla\left(\nabla \cdot \boldsymbol{A}\right) - \nabla^2 \boldsymbol{A}\,, \tag{3}$$

together with Eqs. (1d) and (1a). We obtain:

$$\nabla^2 \boldsymbol{E} - \frac{1}{c^2}\frac{\partial^2 \boldsymbol{E}}{\partial t^2} = 0\,. \tag{4}$$

This is the wave equation of electric field in free space. Taking the curl of both sides of Eq. (1d) and obeying the similar procedure, we get the same wave equation for magnetic field:

$$\nabla^2 \boldsymbol{B} - \frac{1}{c^2}\frac{\partial^2 \boldsymbol{B}}{\partial t^2} = 0\,. \tag{5}$$

Eqs. (4) and (5) are second-order linear partial differential equations, which are typically solved by means of separation of variables. Let's take the electric field as an example:

$$\boldsymbol{E}\left(x, y, z, t\right) = \boldsymbol{E}_r\left(x, y, z\right) \mathrm{e}^{-\mathrm{i}\omega t}. \tag{6}$$

Substituting Eq. (6) into Eq. (4), we obtain the Helmholtz equation of electric field:

$$\nabla^2 \boldsymbol{E}_r + \frac{\omega^2}{c^2}\boldsymbol{E}_r = 0. \tag{7}$$

Benefiting from the linearity of Eq. (4), the superposition principle is valid, which means the sum of any two solutions is also a solution. The physical interpretation of this property is that, the actual EM field inside the cavity is a superposition of some fundamental fields, which are the solutions of Eq. (7). They are named eigenmodes, because each of them has a certain angular frequency ω and a certain field pattern $\boldsymbol{E}_r$. The particular superposition coefficients of eigenmodes finally determine the actual EM field.

[1] The reality is that the EM field can be excited by couplers, see Sec. 2.2.3.

Because the simple boundary in our case is cylindrical, the field pattern can be solved analytically. It is convenient to use cylindrical coordinate. One set of solutions which will benefit to the succeeding discussions are transcribed as follows [4]:

$$E_r = -E_0 \frac{k_z}{k_r} J_n' \left(k_r r\right) \cos n\theta \sin k_z z \, \mathrm{e}^{-\mathrm{i}\omega t} \,, \tag{8a}$$

$$E_\theta = E_0 \frac{n k_z}{k_r^2 r} J_n \left(k_r r\right) \sin n\theta \sin k_z z \, \mathrm{e}^{-\mathrm{i}\omega t} \,, \tag{8b}$$

$$E_z = E_0 J_n \left(k_r r\right) \cos n\theta \cos k_z z \, \mathrm{e}^{-\mathrm{i}\omega t} \,, \tag{8c}$$

where $J_n(x)$ is the Bessel function of order n and $J_n'(x)$ is the derivative of $J_n(x)$, k_r and k_z are two constants to be determined by the boundary conditions (2).

Due to the constraints set by the boundary conditions, E_θ and E_z must vanish on the curved wall. If the radius of the cylinder is R, then we require:

$$J_n \left(k_r R\right) = 0 \,, \text{ which gives } k_r = \frac{p_{nm}}{R} \,, \tag{9}$$

where p_{nm} is the mth zero of the nth order Bessel function $J_n(x)$. Besides, we also need $E_r = E_\theta = 0$ on two flat walls, which are placed at $z = 0$ and $z = L$, respectively. L is the height of the cylinder. These conditions are satisfied only if:

$$\sin k_z L = 0 \,, \text{ therefore } k_z = \frac{l\pi}{L} \,, \tag{10}$$

where l is an integer.

For the magnetic field, we can deduce the formulae from the solutions of electric field (8), using relation (1c):

$$B_r = \mathrm{i} E_0 \frac{n\omega}{c^2 k_r^2 r} J_n \left(k_r r\right) \sin n\theta \cos k_z z \, \mathrm{e}^{-\mathrm{i}\omega t} \,, \tag{11a}$$

$$B_\theta = \mathrm{i} E_0 \frac{\omega}{c^2 k_r} J_n' \left(k_r r\right) \cos n\theta \cos k_z z \, \mathrm{e}^{-\mathrm{i}\omega t} \,, \tag{11b}$$

$$B_z = 0 \,. \tag{11c}$$

Note that the longitudinal component of magnetic field is zero, i.e. the magnetic field is purely transverse. As a convention, we usually indicate such modes as TM together with three indices: n (azimuthal), m (radial) and l (longitudinal) and denote them as TM_{nml}. This class of eigenmodes are commonly used for beam diagnostics, as we will explain later.

Combing Eq. (7) and Eqs. (8) gives the angular frequency ω_{nml} of the mode TM_{nml}:

$$\omega_{nml} = c\sqrt{k_r^2 + k_z^2} = c\sqrt{\left(\frac{p_{nm}}{R}\right)^2 + \left(\frac{l\pi}{L}\right)^2} \,. \tag{12}$$

The eigenfrequencies of a cavity are the most important parameters, which are only determined by the geometry of the cavity, as seen from Eq. (12).

2.2 Pillbox Cavity with Pipe

The case that we consider before is a purely mathematical model, but it still lay the foundation of the following discussions. In reality, the cylinder is not a entirely closed space, since the beam pipe has to be taken into account for the traveling path of the beams. Second, the enclosure material of the cavity has finite electric conductivity, thus the EM energy will be eventually converted to heat on the walls. Fortunately in practice, the size of the beam pipe is small compared to the wavelength of employed

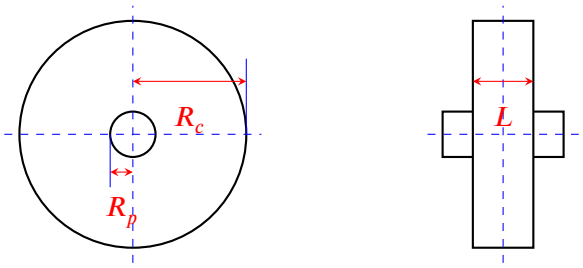

(a) front view (b) side view

Figure 2: Sketch of a pillbox cavity with pipe.

eigenmode, and the highly conductive metals — oxygen-free high conductivity copper, for example — are adopted in the manufacture. As a consequence, these two effects can be treated as perturbations to the ideal model, which makes the solved EM field pattern is still valid to a great extent. With the improved model of pillbox cavity with pipe shown in Fig. 2, we will bring out some other important characteristics of a cavity.

2.2.1 Quality Factor

Since the EM waves can disperse through the beam pipe and dissipate on the walls via heat conversion, the cavity is no longer a lossless system. We shall modify the solutions to Maxwell's equations slightly by introducing imaginary parts to the frequencies to describe damped oscillations of EM waves. Hence each mode will be characterized by its frequency $\omega/2\pi$ and its decay rate α. The field amplitude of a mode will decay exponentially as $\propto \mathrm{e}^{-\alpha t}$, and the stored energy W in the cavity will decay as $\propto \mathrm{e}^{-2\alpha t}$. The *quality factor* Q_0 is defined as the ratio of the stored energy per oscillation cycle to the power loss P_0 [5]. The subscript 0 is to stress that this factor is merely determined by the cavity itself. According to the definition:

$$Q_0 = \frac{\omega W}{P_0} = \frac{\omega W}{-\frac{\mathrm{d}W}{\mathrm{d}t}} = \frac{\omega}{2\alpha}\,. \tag{13}$$

Q_0 describes the lossy character of the cavity. From Eq. (13), it is clear to see that the larger Q_0 is, the slower the EM waves are damped, and thus the smaller will become the power necessary to compensate for the energy losses. For the cavity design, we can tune the cavity to operate around one of its eigenfrequencies and take advantage of high Q_0 by using the resonance phenomenon that will lead to strong EM field.

2.2.2 Shunt Impedance

Because the beam will lose energy when it passes through a cavity, the cavity owns some characters of being a resistor in a circuit. The quantity *shut impedance* R_s is thus to describe the strength that the cavity obstructs the beam. We take the "Linac-ohms" definition of R_s [5]:

$$R_s = \frac{\left|V_{acc}\right|^2}{P_0} = \frac{\left|\int_0^L E_z \mathrm{d}z\right|^2}{P_0}\,, \tag{14}$$

where the accelerating voltage V_{acc} is the integral of the longitudinal component (8c) of electric field along the beam direction.

The shunt impedance is related to the geometry of the cavity, as well as the EM properties of the material. However, the ratio R-over-Q is independent of material, only determined by the geometry and the specific eigenmode. This can be proven by substituting Eq. (14) into Eq. (13):

$$\frac{R_s}{Q_0} = \frac{\left|V_{acc}\right|^2}{\omega W}\,. \tag{15}$$

The material-related dissipation power P_0 is cancelled after calculating the ratio.

In fact, R_s/Q_0 is more often used than R_s, because it allows to separate the material effects in the first place. Due to the same reason, R_s/Q_0 is regarded as a more fundamental characteristics of a cavity and used more often.

2.2.3 Coupler

Sometimes we need to actively feed energy into the cavity, like the case of acceleration cavities, or extract energy out of the cavity, as in the case of CBPM. This is realized by couplers to couple the EM field inside the cavity with the external circuit. According to different kinds of field they couple, couplers (Fig. 3) can be classified to three common types [6]:

Magnetic the coupler is a loop which acts like a magnetic dipole. It interacts with magnetic field in the loop area;

Electric the coupler is an antenna which acts like an electric dipole. It interacts with electric fields on the surface of antenna;

Electromagnetic the coupler is a slot connecting the cavity with a waveguide. It acts like a magnetic and/or electric dipole, depending on which field(s) will leak out through the slot.

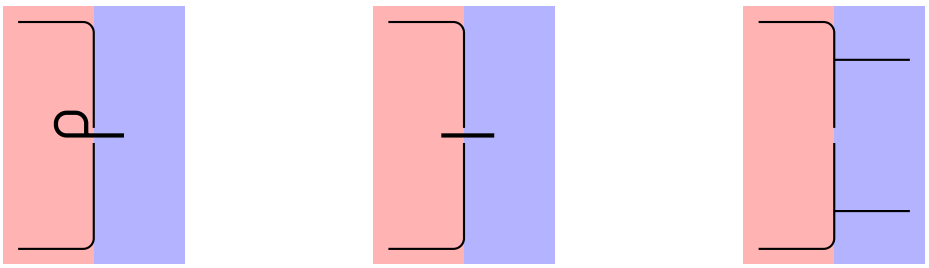

(a) a loop (b) an antenna (c) a slot

Figure 3: Sketch of different kinds of couplers to couple the stored energy of a cavity with external circuits. The red region indicates the cavity, whereas the outside is in blue block.

When the cavity is implanted a coupler, the stored energy is dissipated into not only the cavity wall but also the external circuit. We can define the *external quality factor* Q_{ext} to take external loss power P_{ext} into account.

$$Q_{ext} = \frac{\omega W}{P_{ext}} . \tag{16}$$

The *loaded quality factor* Q_L is naturally defined as:

$$Q_L = \frac{\omega W}{P_0 + P_{ext}} , \tag{17}$$

which leads to the relation of three kinds of Q values:

$$\frac{1}{Q_L} = \frac{1}{Q_0} + \frac{1}{Q_{ext}} . \tag{18}$$

2.2.4 Coupling Coefficient

It is meaningful to evaluate how strong the coupler couples with the EM field. Hence we introduce the *coupling coefficient* β defined as [6]:

$$\beta = \frac{P_{ext}}{P_0} = \frac{Q_0}{Q_{ext}} . \tag{19}$$

The reflection coefficient Γ seen by the signal source under the assumption of zero-electric-length transmission line, is related to β by:

$$\Gamma_{\omega=\omega_{res}} = \frac{\beta - 1}{\beta + 1}, \tag{20}$$

where $\omega = \omega_{res}$ means Eq. (20) is only valid when the cavity is at resonances.

The coupling coefficient plays an important role in the design of a cavity, since it determines the reflection coefficient, and the ratio between the power dissipated into the walls and the external loads. It is possible, in general, to change it by altering the geometry of the coupler.

The particular case of $\beta = 1$ is of great interest, because under this condition, we don't get reflected power at the input port. This is called *critical coupling*, being contrary to under-coupling and over-coupling for $\beta < 1$ and $\beta > 1$, respectively. It is usual to set the coupling to be critical.

2.3 Beam Position Detection

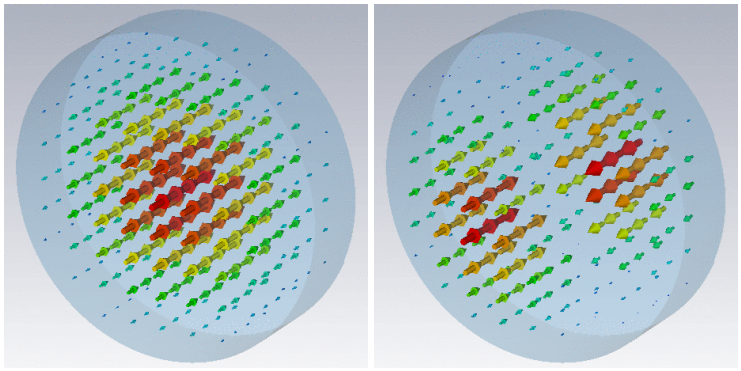

(a) TM_{010} (b) TM_{110}

Figure 4: The electric field patterns of eigenmodes TM_{010} and TM_{110} in a circular cavity.

For beam diagnostics, the two lowest eigenmodes of the circular cavity, namely TM_{010} and TM_{110}, are frequently utilized to measure intensity and position of the beam. Because of the electric field patterns, which are depicted in Fig. 4, they are normally called monopole mode and dipole mode, respectively.

It is a fact that, the electric field of monopole mode mostly concentrates around the center (Fig. 4a), where the field changes steeply for the dipole mode (Fig. 4b). As a consequence, the beam will not feel too much difference if it offsets in the neighborhood of center when the cavity resonates in the monopole mode. However for the dipole mode, the interaction between the beam and the cavity will severely change in the same region. In other words, the dipole mode is sensitive to the beam transverse position, whereas the monopole mode is not. Therefore a CBPM usually operates in the dipole mode, rather than monopole mode to determine beam positions.

Nevertheless, it is worthwhile to mention that the dipole mode is actually degenerated, due to the rotational symmetry of the pillbox. The two degrees of freedom on the transverse plane permit two possible polarizations of dipole mode, whose polarized axes are mutually orthogonal. They are conventionally named as X-polarization and Y-polarization. Since the frequencies of both polarizations are the same, we can not separate them with normal signal processing scheme. To reduce the potential systematic errors introduced by "cross talk" between two polarizations, special techniques must be taken into the cavity design, by deforming the cavity a bit, intruding some obstacles into the cavity, attaching some coupling waveguides, and so forth.

2.3.1 Beam Loading

When a bunch of charged beam enters into the cavity, it will excite EM field inside the hollow space. Meanwhile, the beam will also feel the EM force exerted by the existing EM field, even including the

field excited by itself. This phenomenon is called *beam loading* [7].

The energy flow from beam to cavity, or the other way around, can be presented mathematically in respect of shunt impedance of the cavity. First, let's consider a charged particle that is about to enter a cavity. At this moment, there is no EM field trapped in the cavity yet. After the particle enters, it will excite EM field which is decomposable to the eigenmodes of the cavity. From now on, we will focus on one particular mode to calculate the excited voltage of such mode. The voltages of other modes can be obtained in the same way [8].

Let's assume the charge of the particle is q, the excited voltage of that mode is V_{exc}, at the same time, the particle feels decelerating voltage V_{dec}. V_{dec} should be related to V_{exc} proportionally:

$$V_{dec} = \gamma V_{exc} \,. \tag{21}$$

Next, the second particle comes in and excites its own EM field in the cavity. Since the cavity has already trapped EM field excited by the first particle, the second particle feels stronger decelerating voltage:

$$V_{exc} e^{i\delta} + V_{dec} \,, \tag{22}$$

where the phase δ indicates the oscillation of the EM field during the time interval between two particles.

From beam's point of view, it loses energy of W_{beam}:

$$W_{beam} = q\Re\left\{V_{dec}\right\} + q\Re\left\{V_{exc} e^{i\delta} + V_{dec}\right\} = 2q\gamma V_{exc} + qV_{exc}\cos\delta \,. \tag{23}$$

The accelerating voltage V_{acc}, after two particles have passed, is the sum of the voltage excited by both particles:

$$V_{acc} = V_{exc} e^{i\delta} + V_{exc} \,. \tag{24}$$

Using Eq. (15), the stored energy W_{cavity} can be written as:

$$W_{cavity} = \frac{\left|V_{acc}\right|^2}{\omega\left(R_s/Q_0\right)} = \frac{2V_{exc}^2\left(1+\cos\delta\right)}{\omega\left(R_s/Q_0\right)} \,. \tag{25}$$

Under assumption of lossless system, which requires energy conservation, W_{beam} and W_{cavity} must be equivalent. As a consequence, we have:

$$2q\gamma V_{exc} + qV_{exc}\cos\delta = \frac{2V_{exc}^2\left(1+\cos\delta\right)}{\omega\left(R_s/Q_0\right)} \,. \tag{26}$$

Because of the arbitrary phase δ, Eq. (26) is actually a couple of equations:

$$2q\gamma V_{exc} = \frac{2V_{exc}^2}{\omega\left(R_s/Q_0\right)} \,, \tag{27a}$$

$$qV_{exc}\cos\delta = \frac{2V_{exc}^2\cos\delta}{\omega\left(R_s/Q_0\right)} \,, \tag{27b}$$

which lead to:

$$V_{exc} = \frac{q\omega}{2}\left(\frac{R_s}{Q_0}\right) \,, \tag{28}$$

and $\gamma = 1/2$. The interpretation is quite interesting: for any eigenmode of a cavity, a charged particle only feels half of its exited field. This was originally proven by P. B. Wilson in one of his reports [9], where he called it the *Fundamental Theorem of Beam Loading*.

2.3.2 Output Signal

Eq. (28) shows the exited voltage of one eigenmode is proportional to the eigenfrequency and shunt impedance of that mode. Combining Eq. (28) and Eq. (15) gives the stored energy in the cavity:

$$W = \frac{V_{exc}^2}{\omega\left(R_s/Q_0\right)} = \frac{q^2\omega}{4}\left(\frac{R_s}{Q_0}\right) . \tag{29}$$

From the definition of Q_{ext} (16), the power extracted out of the cavity is:

$$P_{ext} = \frac{q^2\omega^2}{4Q_{ext}}\left(\frac{R_s}{Q_0}\right) . \tag{30}$$

If we dissipate this power by an impedance Z, the voltage of output signal will be:

$$V_0 = \sqrt{Z P_{ext}} = \frac{q\omega}{2}\sqrt{\frac{Z}{Q_{ext}}\left(\frac{R_s}{Q_0}\right)} . \tag{31}$$

In practice, the decay rate α should be taken into account, as well as the oscillation effect. Thus the output signal is actually presented as:

$$V = V_0 \mathrm{e}^{-\alpha t}\cos\left(\omega t + \varphi\right) , \tag{32}$$

shown in Fig. 5.

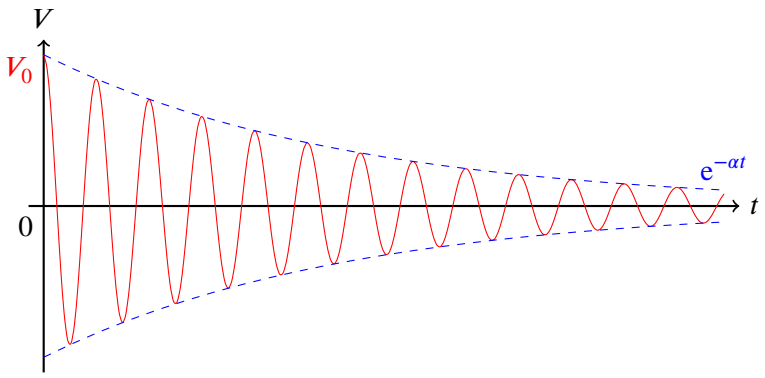

Figure 5: The typical output signal from a cavity.

It is interesting to notice that, from Eq. (31), V_0 is determined by three characteristics of a cavity, i.e. ω, Q_{ext} and R_s/Q_0. When a cavity has been built, ω and Q_{ext} both are fixed and barely change. Yet R_s/Q_0 allows for flexibilities, since it also depends on transverse positions of beams.

Recalling the expression of longitudinal component of electric field in a cylinder (8c), for monopole and dipole modes, E_z take the forms:

$$E_z^{010} = E_0 J_0\left(\frac{p_{01} r}{R}\right)\mathrm{e}^{-\mathrm{i}\omega t} , \tag{33a}$$

$$E_z^{110} = E_0 J_1\left(\frac{p_{11} r}{R}\right)\cos\theta\,\mathrm{e}^{-\mathrm{i}\omega t} . \tag{33b}$$

For the small beam offset from the center, we can expand Bessel functions to the first order as fairly good approximations:

$$E_z^{010} \simeq E_0\,\mathrm{e}^{-\mathrm{i}\omega t} , \tag{34a}$$

$$E_z^{110} \simeq E_0\left(\frac{p_{11} r}{2R}\right)\cos\theta\,\mathrm{e}^{-\mathrm{i}\omega t} = x\frac{p_{11} E_0}{2R}\mathrm{e}^{-\mathrm{i}\omega t} , \tag{34b}$$

where $x = r\cos\theta$ is the projection of beam offset with respect to X-axis.

Substituting Eqs. (34) into Eq. (15), we obtain [8]:

$$\left(\frac{R_s}{Q_0}\right)_{010} \simeq k_{010}\,, \tag{35a}$$

$$\left(\frac{R_s}{Q_0}\right)_{110} \simeq k_{110}x^2\,, \tag{35b}$$

where k_{010} and k_{110} are constants to be determined by the geometry of the cavity. From Eqs. (35), Eq. (31) and Eq. (32), it is obvious to notice that the output signal is independent of beam offset in a small range for the monopole mode, whereas linearly related to the offset for the dipole mode. As a result, the monopole mode is suitable for beam intensity detection but the dipole mode is better for beam position detection.

2.3.3 Signal Contamination

For a CBPM, the ideal signal we want to finally get is Eq. (32), where the amplitude V_0 is proportional to the beam offset x. Thus by measuring the voltage of the signal, we can detect the beam position. However in reality, the situation is more complicated, as the signal is usually contaminated by other sources: monopole mode, beam angle and bunch tilt. In the following, each source will be covered concisely.

Monopole Mode As can be seen from Eqs. (35), for small beam offset x, the shunt impedance of dipole mode is almost zero, which is much smaller than that of monopole mode. This directly results that the signal strength of dipole mode is much weaker. If looking at the resonant spectrum in frequency domain, even though two resonant peaks are spaced apart from each other, the signal tail of the monopole mode extending to the dipole frequency still causes inevitable background. To reduce such effect, two general methods, namely symmetry discrimination and frequency discrimination, are adopted in practice [10]. The former is taking the subtraction of two signals from oppositely placed couplers, and the latter is using a band pass filter centered at dipole frequency.

Beam Angle If the beam travels in a small angle ϕ with respect to the symmetry axis of the cavity, the output signal will get another contribution from this effect. It can be modelled as the sum of two halves offset beams, shown in Fig. 6. One half enters the cavity with offset $-L\phi/4$ and phase $L/4c$, while the other half leaves the cavity with offset $L\phi/4$ and phase $-L/4c$, where we have already adopted the approximation $\tan\phi \simeq \phi$. The sum effect is calculated as:

$$V_{angle} \propto -\frac{L\phi}{4}\cos\omega\left(t+\frac{L}{4c}\right)+\frac{L\phi}{4}\cos\omega\left(t-\frac{L}{4c}\right)=\frac{L\phi}{2}\sin\left(\frac{\omega L}{4c}\right)\sin\omega t\,. \tag{36}$$

Note that the signal caused by beam angle is in quadrature phase with respect to the beam offset signal.

Bunch Tilt It is sometimes possible that the bunch orientates off the trajectory direction by a small angle ψ, even if the beam travels along the longitudinal axis. When the bunch size is comparable to the wavelength of dipole mode, this effect must be taken into account. A new contamination with regarding to the bunch tilt thus appears. We may model this effect by considering two point charges separated by s in longitudinal direction, as shown in Fig. 7. The sum signal V_{tilt} is expressed as:

$$V_{tilt} \propto \frac{s\psi}{2}\cos\omega\left(t+\frac{s}{2c}\right)-\frac{s\psi}{2}\cos\omega\left(t-\frac{s}{2c}\right)=-s\psi\sin\left(\frac{s}{2c}\right)\sin\omega t\,. \tag{37}$$

Again, the signal caused by bunch tilt is also in quadrature phase with respect to the beam offset signal. Therefore, to reduce the effects by beam angle and bunch tilt, a phase detection module is essential for a CBPM system. That is why we usually use a reference cavity working in the monopole mode to calibrate the charge and phase of the beam, together with a position cavity working in the dipole mode.

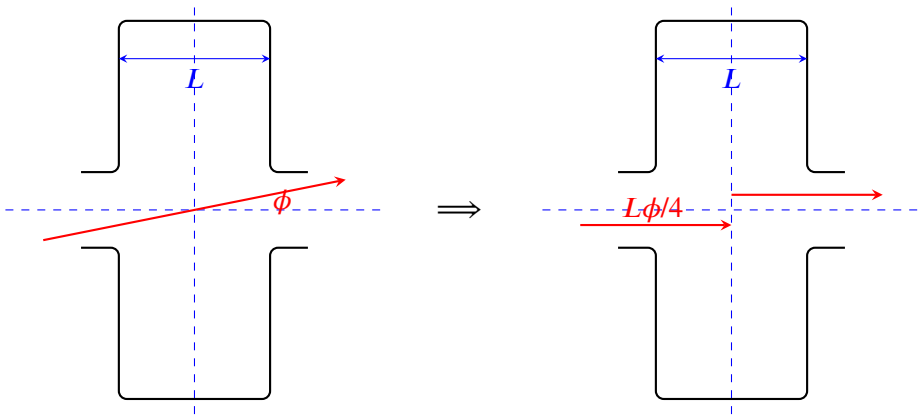

Figure 6: Modelling of a beam passing through a cavity with a small angle.

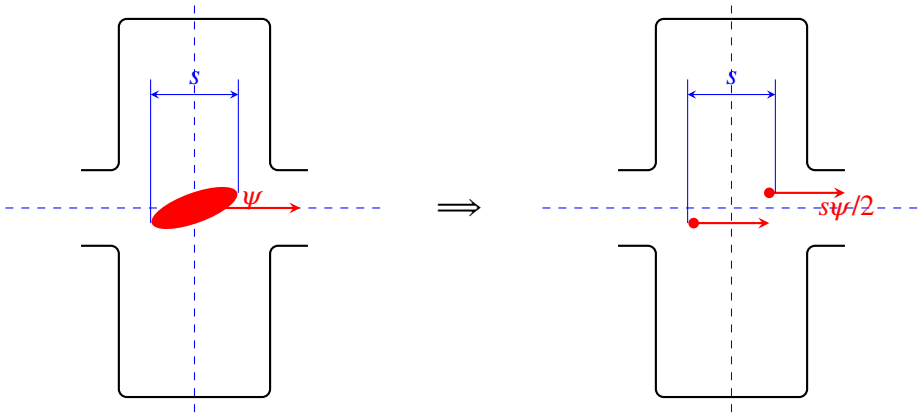

Figure 7: modelling of a tilted bunch passing through a cavity.

3 Diversity of CBPMs

The idea of embracing cavity concept into BPM design to enhance the signal-to-nose ratio was originally brought up by Bergere *et al.* in 1962 [11]. It was an improvement of traditional BPM used in the linear electron accelerator in CEA Saclay[2]. The former one had four loops mounted in the beam pipe and evenly spaced by 90° around the circumference of the cavity. To optimize the sensitivity, a novel design using four resonant cavities instead of loops was proposed. Later in 1963, Neal at SLAC also came up with a similar idea which was reported in [12].

It is visible in Fig. 8 that four identical cavities are mounted on a mechanical support to allow centering around the beam on the transverse plane. On one side of each cavity is a slot used as a magnetic coupler. The induced power in these cavities is picked up by four loops before rectification and further processes. The cavity resonates in monopole mode and is tuned to 3 GHz, which is the acceleration frequency of linac. The unloaded quality factor of the cavity is about 500. This assembly carries an advantage of better sensitivity, which is however traded off by more stringent construction demands, as the cavities must be exactly the same to eliminate systematic errors.

Following the pioneer work at CEA Saclay, more and more CBPMs have come out worldwide in different laboratories. In general, they can be categorized into four major families, namely rectangular, circular, re-entrant and choke mode. In the subsequent sections, each family will be elaborated by existent instances taken from literatures starting from 1960s.

[2]CEA is the acronym for the French research organization: *commissariat à l'énergie atomique*. CEA Saclay is one of its research centre on the Saclay plateau.

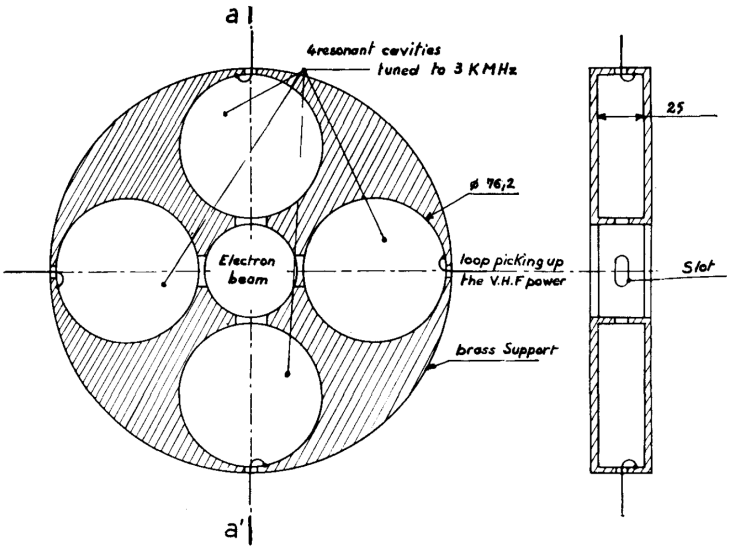

Figure 8: Front cut view (left) and side cut view (right) of the resonant CBPM designed at CEA Saclay in 1962. *Taken from* [11].

3.1 Rectangular Cavity

Back to 1961 when SLAC was approved by the Congress, physicists were awaiting the commission of Standford two-mile linear accelerator. For this complex facility, BPM system is of crucial importance. Several designs have been proposed by Brunet *et al.* in 1964 [13], including traveling wave monitor, resonant ring, shorted waveguide and cavity. Finally a rectangular cavity was adopted and later published by Farinholt *et al.* in 1967 [14]. This is the world's first rectangular cavity used for monitoring beam positions in an accelerator, which marks the beginning of history of CBPMs.

The monitoring system was installed at the beam switch yard of beam line. Each monitor assembly comprised two perpendicularly placed rectangular cavities operating in TM_{120} mode[3], and one circular cavity operating in TM_{010} mode. The position cavities operated at frequency of 2856 MHz — equal to the acceleration frequency of linac. The loaded quality factor is 325 [13]. According to the performance report by Farkas *et al.* [15], the CBPM achieved position resolution of 10 µm at beam intensity of 100 µA, 1 mm at 100 nA.

In 1987, almost 20 years later, Goldberg *et al.* also built a rectangular CBPM for the Tevatron at Fermilab [16]. The rounded corner cavity worked in dipole mode at frequency of 2044.5 MHz. This frequency was chosen to be a half-integer multiple of the RF frequency to minimize possible coherent signal contamination in multibunch operation. Besides, the actual resonant frequencies of X- and Y-cavities were intentionally displaced by ±2 MHz from the calculated frequency. The splitting should be low enough to allow for reasonably narrow bandwidth of signal processing electronics, yet high enough to avoid incidental coupling between the two cavities. The Q_0 was chosen to be 10 000 at design stage, then tested to be 9500 and 9200 for each cavity after fabrication.

As an example of next generation of accelerators, the proposed International Linear Collider (ILC) has been catching physicists' more and more attentions since 1990s. To achieve high luminosity collision, ILC requires beam size of a few nanometers and beam stability of the same scale. For this purpose, Inoue *et al.* at KEK[4] developed a high resolution CBPM (Fig. 9) and tested it at the focal point of ATF2 [17]. The system demonstrated 8.7 nm position resolution over a dynamic range of 5 µm with beam intensity of $\sim 10^{10}$ e/bunch. The rectangular cavity was designed to have different length and width, in order to well isolate X and Y position signals. As a result, the eigenfrequencies of X and Y dipole modes are

[3]The notation TM_{nml} of a rectangular cavity is similar to that of circular one. n, m and l indicate the number of extremes of electric field counted along axis x, y and z, respectively.

[4]KEK is the acronym for the Japanese organization *kō-enerugī kasokuki kenkyū kikō*. It focuses on high energy research.

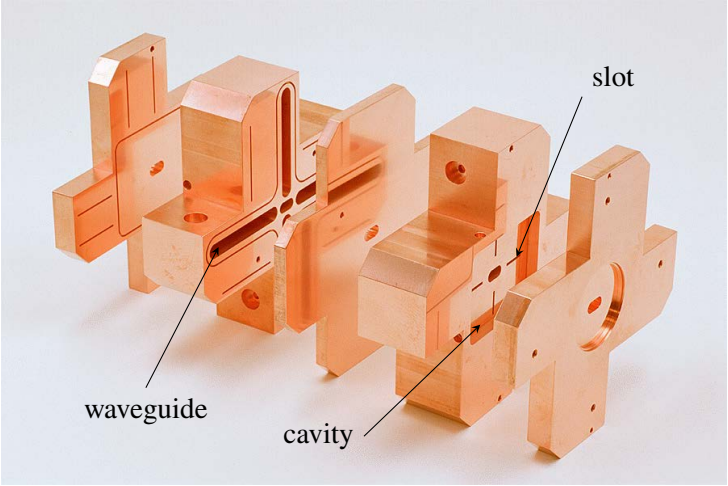

Figure 9: Structure of CBPM block designed at KEK in 2008. *Taken from* [17].

5.712 GHz and 6.426 GHz, respectively. The signals are coupled out through slots located in the cavity's end plate. The coupling coefficient was carefully set to 1.4 for X-ports and 2.0 for Y-ports, since higher coupling increases sensitivity, yet reduces dynamic range by saturating the electronics. The waveguides can resonate dipole mode, as well as reject monopole mode by setting the cutoff frequency of waveguide between frequencies of monopole and dipole.

Another example of rectangular CBPM was made by Su *et al.* at Tsinghua University [18]. The cavity was installed in TTX to monitor beam transverse positions. The configuration is very similar to the above Japanese one, using four waveguides to extract beam induced signals. The cold test frequencies are 5.6618 GHz and 5.7794 GHz respectively for X- and Y-cavities. And measured Q_0 is about 6500 while the required value is 9700. However after welding, the value increases to ~8000, which nearly satisfies the requirement.

3.2 Circular Cavity

Among all types, the circular one is the most widely used, not just because the RF properties can be precisely understood by analytic methods, but also it can be easily manufactured. The world's first circular CBPM was developed by McKeown at CRL in 1979 [19]. The cavity was tuned to 2.415 GHz — the third harmonic of acceleration frequency. As shown in Fig. 10, it was constructed to meet quadrupole symmetry by introducing tuning plungers at radial positions near the electric field maximum. This symmetry was maintained by four magnetic coupling loops on the circumference. After the cavity was built, the beam tests were carried out in the beam line of ETA. The electron beam was held steady at about 1 mA, while the cavity moved horizontally and vertically. The position sensitivity was obtained as $0.35\,\mathrm{mW}^{1/2}\,\mathrm{mm}^{-1}\,\mathrm{mA}^{-1}$. As a continuation of McKeown's work, Chan *et al.* developed another CBPM with small modifications 2 years later [20]. Fist the resonant frequency was set to the fourth harmonic of acceleration frequency. Second the electric probes were used as coupler instead of magnetic loops.

Similar to ILC, the compact linear collider (CLIC) is also a proposed electron-positron collider in the post-LHC era for physics up to multi TeV center-of-mass colliding beam energy range. A big collaboration based at CERN[5] have been working on this project since early 1990s. In 1992, Schnell *et al.* reported the development of CBPM to be used in CLIC [21]. The successful operation of CLIC will demand μm precision measurements of transverse beam position along the full length of the main linac. The resonant frequency of CBPM was tuned to 33 GHz, slightly above the acceleration frequency of 30 GHz, so as to

[5]CERN is the acronym for the French *conseil europen pour la recherche nuclaire*. At that time when it was founded, the most frontier of physics was to study the inside of the atom, hence the world *nuclear*. Today, CERN has become the world's centre of particle physics, dedicated to the study of the fundamental constituents of matter and the forces acting between them.

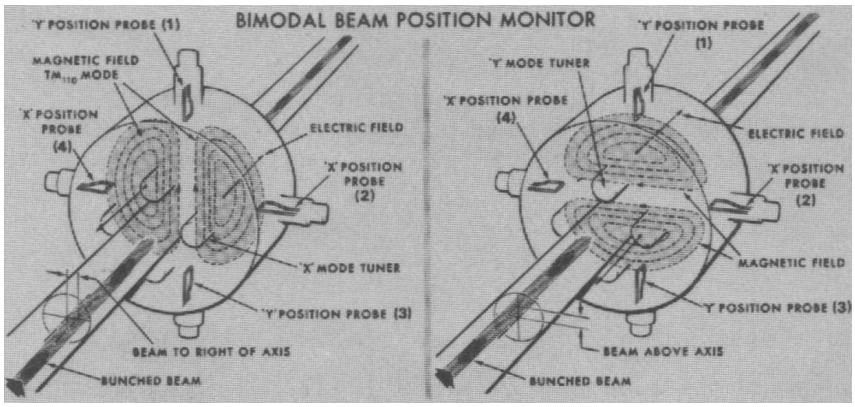

Figure 10: Bimodal CBPM designed at CRL in 1979. X- and Y-dipole mode can be switched by tuning plungers. *Taken from* [19].

reduce the risk of interference by the power pulse. A prototype was tested in CTF using 50 MeV, 1 nC single bunch beam. The test setup consisted of a reference cavity and two position cavities, which were mounted on 0.1 µm resolution micro-movers for displacement calibration. The upper limit on CBPM resolution derived from measurement results was 4 µm, as reported by Sladen *et al.* in 1996 [22]. However, the authors also pointed out, "…the true BPM resolution is almost certainly in the nanometer range and these results are probably an artifact of specific beam conditions."

Almost at the same time, Euteneuer *et al.* at University of Mainz presented beam monitors at MAMI [23]. The design goal of position monitoring was to distinguish beam deviations of 0.05 mm at current of 1 nA, corresponding to cavity power around 10^{-18} W. To increase the sensitivity, the mode stabilizers in the circular cavities were built as capacitive cylinders, drawing the electric field maxima inwards. By the steeper gradient of the electric field, the shunt impedance can be enhanced by up to a factor of 5. To achieve high time resolution of 12 ns, low $Q_L \sim 30$ was chosen.

Inspired by the CBPM idea of Hayano and Shintake, which was originally designed for JLC [24], Lorenz and Yezza at Technical University of Berlin built a circular cavity for TESLA in 1993 [25]. Because the theoretical resolution of CBPM is limited by monopole mode excitation, a ring combiner was attached to the cavity to reject such mode (Fig. 11). A symmetry rejection of more than 30 dB for monopole mode was expected. A selective coupler located at the point where the magnetic field of dipole mode is zero was also adopted in the design. The CBPM was installed in TTF, and tested at room temperature. The resonant frequency was 1.517 GHz, coupling coefficient was 0.95, and unloaded quality factor was 3025 [26].

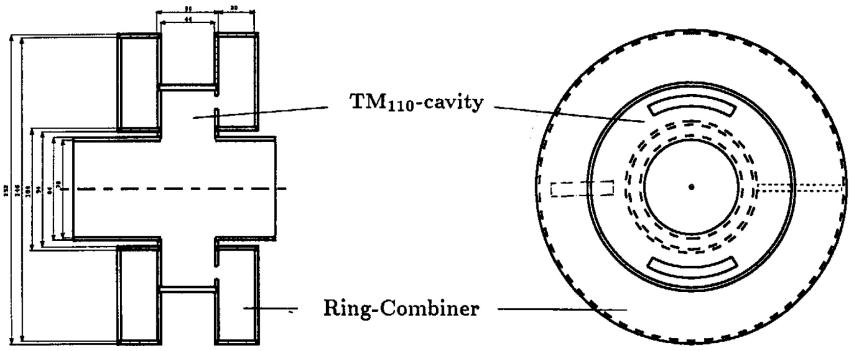

Figure 11: Sketch of CBPM with a coaxial ring combiner designed for TESLA in 1993. *Taken from* [25].

Another group led by Balakin at BINP also demonstrated a CBPM system with sub-micron position resolution in 1994 [27]. The designed CBPM was expected to be sensitive to about 0.1 µm to meet the

requirement of VLEPP[6] project. In fact the obtained sensitivity being able to detect signal in order of 10^{-11} W corresponds to a few nanometers of VLEPP beam's offset. The prototype is very similar to the above one, which also connects with a ring combiner by two symmetric coupling slots. Output power is extracted from the ring combiner through coaxial plug. Additional coaxial cavity with very low Q_0 (loaded by ferrite) is mounted nearby and used for damping of parasitic modes. On the bench top, the resolution of this system was measured as 0.05 µm. Five years later, the CBPM was installed in ATF at BNL, and tested with 0.25 nC bunch charge beam. A position resolution of 0.15 µm was obtained [28].

Due to some financial problems happened to BINP, unfortunately VLEPP could not be realized. Then the Russian group joined ILC collaboration, and developed another CBPM operating at 6429 MHz [29]. According to a paper published in 2007 by Walston *et al.* [30], the position resolution of such cavity was 15.6 nm and the tilt resolution was 2.1 µrad over a dynamic range of almost ±20 µm. The dipole mode excited in the cavity was selectively coupled out by two orthogonal slots. These slots — one each for X and Y directions — exploited the difference in the field pattern of monopole and dipole modes to reject the tails of monopole signal with frequency at dipole resonance.

In 1997, Ursic *et al.* at JLab developed a CBPM system to measure transverse position of very low current beams delivered to the experimental hall B of CEBAF [31]. In the heart of such system was a position cavity operating at 1.497 GHz, which was the third harmonic of bunch frequency. The loaded quality factor was 3500, and the sensitivity was 70 pV/µm at beam current of 1 nA. The system was capable of handling wide dynamic range of beam currents from nA to µA with an expected resolution better than 100 µm. The position cavity is equipped with field perturbing rods, which draw the electric field maxima of dipole mode closer to the center. As a consequence, the rods increase the resolution by a factor of 2.5, reject cross talks between X and Y polarizations, and introduce loss, deteriorate quality factor. The resulting broader resonance peak is then beneficial in reducing drifts for improved long term measurement stability.

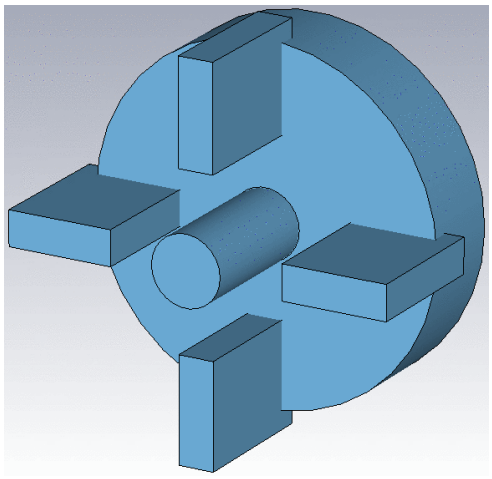

Figure 12: 3D model of a dipole selective cavity coupled with four waveguides.

One particular configuration of circular CBPM, which is shown schematically in Fig. 12, is more and more frequently used in various accelerators. The resonant dipole field in the cavity is coupled with four symmetrically placed rectangular waveguides. This special design takes advantage of difference in EM field distributions of monopole mode and dipole mode. In the intersecting area of cavity and waveguides, the magnetic field lines of monopole mode and dipole mode are almost perpendicular to each other. Because the dipole field points to the preferred propagating direction of waveguide, it can easily enter the waveguide, whereas the monopole field is rejected outside. By installing antennas in the waveguides, a considerable suppression of monopole signal with respect to dipole can be achieved. As a

[6]VLEPP is the acronym for the Russian *vstrechniye lineyniye electron-positronniye puchki*, or *встречные линейные электрон-позитронные пучки* in Cyrillic script.

consequence, this configuration of CBPM is often named as "dipole selective" cavity. In 2002, Johnson *et al.* at SLAC first built such cavity resonating at 11.424 GHz to fulfill requirements of proposed NLC [32]. The measured Q_0 was 590, and dipole frequency was 11.45 GHz [33].

Liapine at Technical University of Berlin adopted the same idea as Johnson's to design a cavity for the energy spectrometer in TESLA [34]. The operating frequency was chosen to be 1.518 GHz, a compromise between cavity size and prices of electronic components. The cavity dimensions were carefully selected such that the shunt impedance has the highest possible value and the monopole eigenfrequency is far from acceleration frequency to avoid resonance. The position resolution was tested to be 470 µm for X direction and 203 µm for Y direction in the dynamic range of $\pm$1 mm [35].

Ever since Liapine got his doctoral degree, he moved to UCL in 2005 and has used Lyapin as an alternative spelling. Two years later together with his colleagues, Lyapin presented a new design of CBPM for ESA at SLAC [36]. The CBPM system consisted of three circular cavities designed for use in the cryogenic regions of the ILC linac [37]. The coupler using combination of slots and waveguides provided very good suppression of parasitic monopole mode. These cavities have a low $Q_L \sim 500$ and therefore a short decay time of dipole signal to provide bunch-to-bunch position measurements in ILC without the need to exclude the contaminations from previous bunches. The measured resolution of X-cavity was 0.53(5) µm and that of Y-cavity was 0.46(2) µm. They were significantly worse than predictions, but in reasonable agreement with the amount of vibration recorded by the interferometer, which indicated that the resolutions were limited by mechanical motions.

In 2009, Lyapin *et al.* developed two CBPMs working at different frequencies for ATF at KEK [38, 39]. All the design details and test results of the CBPMs were published by Kim *et al.* three years later [40]. The C-band cavity worked at 6.423 GHz with Q_L of 6000. The position resolutions were measured to be 248 nm for X direction and 254 nm for Y direction. The S-band cavity worked at 2.888 GHz with Q_L of 1800. The position resolutions were measured to be 1.48 µm for X direction and 0.92 µm for Y direction.

Then in 2012, the same UK group contributed another CBPM system for CLIC, and tested it in CTF [41, 42]. The dipole frequency of 14.99 GHz is close to 14 GHz which will be used for RF acceleration in CLIC. As a result, the signals from consecutive bunches add up constructively and dominate signals among other parasitic modes excited by beams. The unloaded quality factor was designed to be 450 such that the signal from any bunch has decayed by a factor of order 10^3 within the time resolution. The signals were extracted via feedthrough antennas at the end of waveguides connected with the cavity.

As a member of both collaborations CLIC and ILC, Fermilab also developed CBPM systems according to the particular requirements of these two projects [43]. The proposed CBPM design is based on a selective mode coupling idea realized in X-band. This schema provides a high spatial resolution while keeping in compact dimensions. In order to measure the beam trajectory within 50 ns time scale, the stainless steel material was used to lower quality factor. The designed dipole frequency was 14 GHz and $Q_0 = 465.5$.

The CBPM that Fermilab designed for ILC operating in L-band at 1.3 GHz and in cryogenic temperatures [44]. The resonant frequency was chosen in a way that signals will be maximized in multi-bunch operation scenario. However this frequency is the same as the acceleration frequency, therefore efficient shielding is mendatory. The cavity is coupled with four waveguides via slots to damp monopole mode. Besides, four antennas are plugged in one flat end of the cavity to directly extract monopole signal, saving an extra reference cavity [45]. After test, Q_L was about 600 and the sensitivity was 0.24 V nC^{-1} mm^{-1} [46].

Meanwhile, an independent group at ANL designed a high resolution X-band CBPM system for LCLS in 2006 [47]. The resonant frequency was 11.384 GHz, Q_L was 3550. The dipole selective CBPM was mounted on a precise 2-axis translation stage, and tested in ITS. With beams of 1 nC single bunch charge and 3 ps bunch length, the sensitivity was measured to be 1.22 mV µm^{-1} nC^{-1}.

In Japan, Maesaka *et al.* at RIKEN[7] published an article recently, reporting a sub-micron resolution

[7] RIKEN is the acronym for the Japanese *rikagaku kenkyūjo*. It is a large nature science research institute in Japan.

CBPM system developed for the SACLA XFEL facility [48]. The resonant frequency is 4.76 GHz for both position cavity and reference cavity. This frequency is intentionally shifted from acceleration frequency so as to reject any backgrounds owing to dark current synchronized with RF field. A low Q_0 of 642(32) is due to the stainless steel material used for construction. Nevertheless, this value is adequate since the coupling coefficient is much greater than unity, thus most of stored energy in the cavity is extracted from the coupling slots. Besides, there are also other advantages for a low Q_0 cavity: the RF phase shift due to temperature drift is small, and the pulse response is relatively fast. The CBPM has been tested with electron beams of 0.1 nC bunch charge and 7 GeV beam energy. The position resolution in the undulator section is less than 0.6 µm. For the low charge operation of beam line, say 0.01 nC, the resolution of 6 µm is obtained.

In collaboration with the Japanese group, Lipka *et al.* at DESY also built some CBPM prototypes for the European XFEL [49]. The design was originally based on the Japanese cavity, then changed according to the boundary conditions of the European XFEL. Two generation of prototypes were constructed. The first one worked at 4.4 GHz, while the second one operated at 3.3 GHz. The lower resonant frequency was later chosen to adapt to the larger beam pipe. Both types were installed in FLASH.

In 2012, a highly sensitive CBPM system that can monitor pA electron beams was developed by Pusch *et al.* at University of Bonn [50]. It was designed for the fixed target experimental setup in ELSA, especially when polarized beams were used. The operation frequency was chosen to be at the third harmonic of bunch frequency of 499.67 MHz. To extract the position signal, two coupling antennas were installed somewhere in the top cap of the cavity. The locations where the electric field of dipole mode reaches its maximum were chosen, based on the analytic evaluation of an ideal cylinder. On the bottom of the cavity, exactly opposite to the coupling antennas, small capacitive cylinders were mounted in order to concentrate the field in their vicinities. The position resolution of 50 µm was achieved.

In the same year, Dal Forno *et al.* at Elettra published their work on CBPM for the XFEL facility in Italy [51]. The dipole mode resonates at 6.5 GHz. The position signals are selectively extracted by four rectangular waveguides, which are magnetically coupled to the cavity. The system has been tested with electron beams with bunch charge of 270 pC and pulse duration of 10 ps. The sensitivity of 0.33 V nC^{-1} mm^{-1} for X-cavity and 0.3 V nC^{-1} mm^{-1} for Y-cavity were obtained.

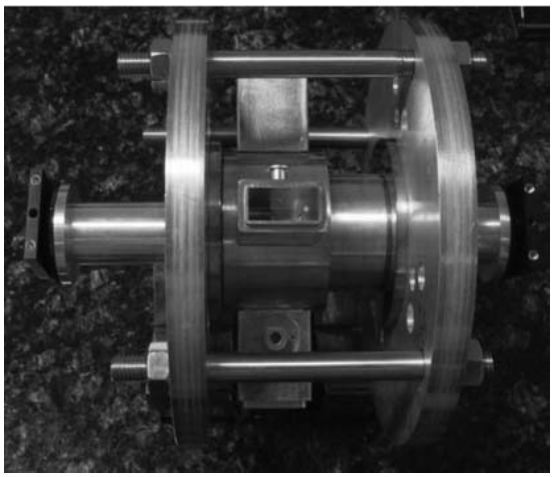

Figure 13: Photo of a prototype CBPM developed at SINAP in 2008. *Taken from* [52].

In Shanghai, China, SDUVFEL facility has been approved by Chinese government. As a result, a new BPM system is needed for the beam alignment. Chu *et al.* at SINAP described bench top measurements of a C-band CBPM in 2008 [53]. For monopole mode rejection, a different coupling scheme was used, as shown in Fig. 13. The two polarizations of dipole mode are coupled magnetically with four waveguides spaced by 90° around the circumference of the cavity. The propagating eigenmodes of the waveguide do not have azimuthal magnetic field in the region of coupling slot, hence the monopole mode is barely

coupled. Via test, Q_0 was measured to be 10 377, close to the designed value of 11 035. The position resolution of the cavity was 2.8 µm.

Finally we would like to mention a group at Technical University of Darmstadt who are working on a similar topic to ours. Their objective is to develop a BPM system for the proposed CR at FAIR. Based on the conference proceeding lately presented by Hansli *et al.* [54], the main structure of the cavity is a pillbox. On its circumference, two selective coupling waveguides are connected oppositely to the cavity (Fig. 14). This particular configuration is able to extract monopole signal and dipole signal simultaneously with specially placed couplers. A magnetic coupling loop at the zero-plane of the dipole mode is used to exclusively couple with the monopole mode, while the attached waveguides are utilized to extract dipole mode. To verify this idea, they have built a simplified demonstrator, and measured its RF properties. The monopole frequency is 1.86 GHz and the dipole frequency is 2.77 GHz for the demonstrator.

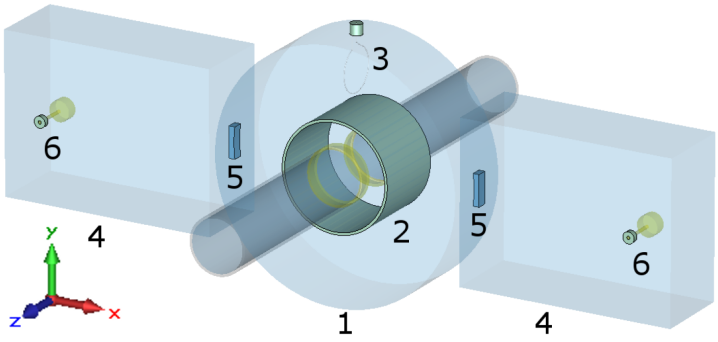

Figure 14: 3D model of a CBPM designed at TU Darmstadt in 2013. The dipole signal is extracted by waveguides, while the monopole signal is couple with a loop (position 3). *Taken from* [54].

3.3 Re-entrant Cavity

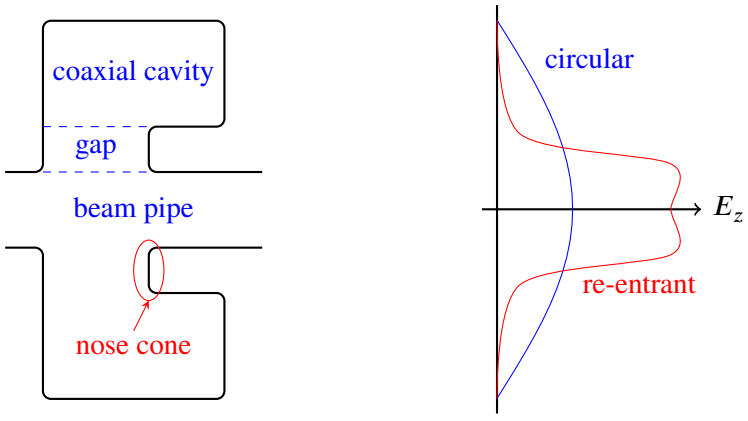

(a) Side cut view of a re-entrant cavity.

(b) comparison of electric field distributions inside a circular cavity and a re-entrant cavity. *Redrawn from* [55].

Figure 15: Schematic plots of a re-entrant cavity and its electric field distribution.

Back to 1964, Altenmueller and Brunet at SLAC first introduced re-entrant shape of cavity when they discussed its EM field distribution [55]. The cavity is a modification of circular one by pushing the margin of one cap outside, the residual portion — called "nose cone" — is thus re-entrant. The structure consists of three distinct regions (Fig. 15a): beam pipe, gap and coaxial cavity [56]. As can be seen from Fig. 15b, the electric field is prominently concentrated in the vicinity of beam pipe by the nose cone [55].

Therefore this special structure will considerably increase the shunt impedance, thus the sensitivity, of the cavity in the central region. Because of such advantage, re-entrant cavities have been often used as beam current monitors to measure intensities, and in klystron tube amplifiers for beam modulations.

The first re-entrant cavity used as beam position monitor was presented by Bossart at CERN in 1994 [57]. For the SPS, eight CBPMs of re-entrant shape working at 200 MHz have been deployed since 1975. During operations, the beam bunches will excite an evanescent dipole mode TE_{11} in the coaxial cavity proportional to the transverse beam displacement off the central axis. For the beam monitoring over a broad bandwidth, typically ~ 100 MHz, the evanescent field is used taking advantage of bandwidth which is a half of the resonant frequency.

Later in 1998, another re-entrant CBPM was built by Magne *et al.* at CEA Saclay and tested in TTF [58, 59]. The position signals were extracted by four symmetrically arranged feedthroughs at the end of coaxial cavity. The measured resolution was 10 µm for a low current beam of bunch charge 1 nC, and the expected resolution was 700 nm for a high current beam. The sensitivity of 0.26 mV mm^{-1} mA^{-1} was obtained.

Several years later, the same group led by Simon published an article on CBPM, in which design, fabrication and beam test of a new re-entrant cavity for the European XFEL was described [60]. This CBPM was designed to be inserted in a cryomodule, working at cryogenic temperatures in a clean room environment. The prototype was installed in FLASH, tested with beam, and the resolution of approximately 4 µm over a dynamic range ± 5 mm in single bunch, resonant frequency of 1724 MHz was obtained.

In 2003, Lorenz *et al.* designed a re-entrant cavity to measure beam alignments at the undulator section of TTF at DESY [61]. The configuration of CBPM system is sketched in Fig. 16. Each cavity is connected to beam pipe via a nose cone, which is benefit to reducing interference between the EM field inside the cavity and that of subsequent bunches. The combination of two independent cavities eliminates incidental cross talks. To each cavity connect two waveguides on the circumference in the opposite directions. The coupling irises between the cavity and the waveguides are designed such that β is 2.5, and Q_L is about 1000. The dynamic range of this system was tested linearly for bunch charges from 0.5 nC to 3 nC.

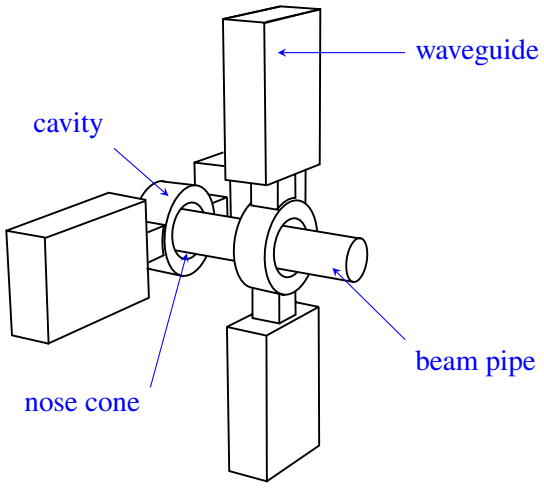

Figure 16: Sketch of CBPM system designed for TESLA in 2003. The system consists of two identical parts which are perpendicular to each other. *Taken from* [61].

In China an S-band re-entrant CBPM system has been designed for a new high brightness injector at HLS by Luo *et al.* at USTC [62]. Coupling waveguides and coaxial probes are installed to extract dipole signals. Through a bench top measurement, the resonant frequency is 2448 MHz and loaded quality factor is 146. The position resolutions are 1.91 µm in X direction and 2.05 µm in Y direction.

3.4 Choke Mode Cavity

As already explained in the theoretical part of this report, the EM field inside a cavity excited by a charged particle can be decomposed into infinite eigenmodes. Each mode interacts with the particle distinctively. One major problem in the RF cavity design that we have always been facing to is how to suppress or damp parasitic modes which are not helpful or even harmful to the cavity operation. According to the application of a cavity, the parasitic modes differ from case to case. For instance, the monopole mode is parasitic for beam position monitors, whereas the dipole mode is parasitic for beam current monitors. The configuration of a cavity should be adapted to the design purpose, in order to feature the desired mode.

In 1992, Shintake at KEK came up with an exceptional idea and proposed a novel design of cavity, namely choke mode cavity, to trap the desired mode and damp the parasitic modes [63]. The geometry of such cavity is shown in Fig. 17. The choke structure is serially mounted on the radial line at a quarter wavelength of the desired mode from the cavity. This special shape will efficiently damp high order modes while keep the desired mode trapped in the cavity. The imaginary part of impedance there becomes infinitely large at the frequency of trapped mode, and thus the real part becomes negligibly small. As a consequence, the RF power of that mode is reflected back to the cavity without losing its energy.

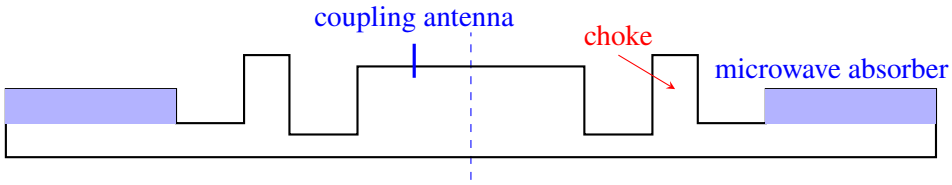

Figure 17: Side cut view of a model choke mode cavity designed at KEK in 1992. The beam pipe is omitted. *Modified from* [63].

Three years later, Shintake's idea was successfully implemented by a CBPM system installed in FFTB [64–66]. The dipole frequency was designed to be 5712 MHz and loaded quality factor was measured to be 130. Using the 47 GeV electron beam provided by FFTB, the choke mode CBPM was tested with single bunch charge of 1 nC. The sensitivity was 25 μV nC^{-1} nm^{-1}, and the resolution was 25 nm.

4 Summary

Beam position monitoring is crucial for the routine operation of any accelerator. Among all the types of BPM systems, cavity beam position monitor is of great importance, owing to its advantages of high sensitivity and sharp resolution. These specifications make it a promising candidate to satisfy strict requirements on beam monitoring and detection demanded by accelerators. Therefore the CBPM system has been investigated and implemented widely since early 1960s. The structures of cavities can be classified as rectangular, circular, re-entrant and choke mode. The circular type is exemplified with great effort, meanwhile the other three are also covered thoroughly. In order to present a comprehensive overview of the evolution history of CBPM during the last half century, various implementations of CBPM are tabulated in Tab. 1, sorted by year. For more information, a complete set of cited references is listed in the last column.

Table 1: Comparison of various CBPMs designed at difference research organizations all over the world.

year	designed at[8]		used in	type	$\varnothing_{cav}$[9] [mm]	L_{cav} [mm]	$\varnothing_{pipe}$ [mm]	f [GHz]	Q[10]	R/Q [$\frac{\Omega}{mm^2}$]	testing beam[11]	resolution[12]	references
1962	CEA Saclay	FR	linac	circular	—	—	—	3	500	—	—	—	[11, 12]
1964	SLAC	US	drift section	rectangular	106.22X 119.58Y	50.83	20.32	2.856	(325)	—	100 nA	1 mm	[13–15, 55, 67]
1979	CRL	CA	ETA	circular	147.5	60	38	2.415	—	—	1.5 MeV 1 mA	(0.35 $\frac{mW^{1/2}}{mA\,mm}$)	[19, 20]
1987	Fermilab	US	Tevatron	rectangular	—	—	—	2.0425X 2.0465Y	9200X 9500Y	29	—	—	[16]
1992	CERN	CH	CTF	circular	10.6	3.56	4	33	(4000)	—	50 MeV 1 nC	< 4 µm	[21, 22, 68–72]
1992	Uni. Mainz	DE	MAMI	circular	141	30	20	—	(30)	—	—	—	[23]
1993	TU Berlin	DE	TTF	circular	235.2	52.5	59.5	1.517	3025	—	cold test	5 µm	[24–26, 73–77]
1994	BINP	RU	ATF@BNL	circular	—	—	—	13.566	—	—	45 MeV 0.25 nC	0.15 µm	[27, 28]
1994	CERN	CH	SPS	re-entrant	338	182	270	0.2	—	—	—	—	[56, 57]
1995	KEK	JP	FFTB	choke mode	120.14	5	40	5.712	(130)	22	47 GeV 1 nC	25 nm	[63–66]
1997	JLab	US	CEBAF	circular	190	95	30	1.497	(3500)	—	1 nA	< 100 µm	[31, 78]
1998	CEA Saclay	FR	TTF	re-entrant	200	50	78	1.658	—	—	3.2 nC	10 µm	[58, 59]
2002	SLAC	US	NLC	circular	29.43	3	12	11.45	(590)	—	—	100 nm	[32, 33, 79–81]
2002	TU Berlin	DE	ELBE	circular	222	18	78	1.518	1680	0.047	15 MeV 50 pC	470 µmX 203 µmY	[34, 35, 82–84]
2003	BINP	RU	ATF@KEK	circular	54.12	12	20	6.429	6950	1.24	1.28 GeV 1.12 nC	15.6 nm	[29, 30, 85–88]
2003	TU Berlin	DE	TTF	re-entrant	21.2	5.2	9.5	12.01	(900)	—	3 nC	< 5 µm	[61]

[8] institute or university followed by two-letter country code
[9] X and Y indicate specified directions for rectangular cavities
[10] unloaded Q_0; parentheses for loaded Q_L
[11] all the testing beams are electron beam
[12] sensitivity is given in parentheses instead, if resolution is not applicable

year	designed at	used in	type	$\varnothing_{cav}$ [mm]	L_{cav} [mm]	$\varnothing_{pipe}$ [mm]	f [GHz]	Q	R/Q [$\frac{\Omega}{mm^2}$]	testing beam	resolution	references
2006	Fermilab	US NML	circular	226	15	78	1.3	5750	14	40 MeV 44 pC	< 1 µm	[44–46]
2006	ANL	US ITS	circular	29	3	10	11.359	(2500)	2.28	200 pC	200 nm	[47, 89–92]
2007	UCL/RHUL	GB ESA	circular	123.61	25	30	2.859	(500)	0.26	28.5 GeV 2.56 nC	0.53 µmX 0.46 µmY	[36, 37, 93]
2008	KEK	JP ATF@KEK	rectangular	60.88X 48.57Y	5.8	6X 12Y	5.712X 6.426Y	5100X 4800Y	0.549X 1.598Y	1.3 GeV 1.1 nC	8.72 nm	[17, 94–97]
2008	CEA Saclay	FR FLASH	re-entrant	99	8	78	1.724	(59)	0.011	1 nC	8 µmX 4 µmY	[60, 98–101]
2008	SINAP	CN SDUVFEL	circular	60.8	20	—	5.712	10 377	—	100 pC	2.8 µm	[52, 53, 102]
2009	UCL/RHUL	GB ATF@KEK beam line	circular	53.8	12	20	6.423	(6000)	1.4	1.3 GeV 1.6 nC	250 nm	[38, 40, 103–106]
2009	UCL/RHUL	GB ATF@KEK final focus	circular	235.2	12	40	2.888	(1800)	0.15	1.3 GeV 1.6 nC	1 µm	[39, 40, 103–108]
2009	DESY	DE FLASH	circular	—	—	—	3.3	—	—	—	—	[49, 109]
2009	Fermilab	US CTF	circular	22.44	2	8	14	(250)	3	—	—	[43, 110, 111]
2010	USTC	CN HLS	re-entrant	95.8	10	35	2.448	(146)	—	cold test	1.91 µmX 2.05 µmY	[62, 112–114]
2011	TU Darm.	DE CR	circular	960	200	400	0.33	(180)	0.005	—	—	[54, 115–117]
2012	RHUL/UCL	GB CTF	circular	—	—	8	14.993	306	—	—	—	[41, 42]
2012	RIKEN	JP SACLA	circular	—	—	20	4.758	642	0.51	250 MeV 0.3 nC	0.198 µmX 0.171 µmY	[48, 118, 119]
2012	Uni. Bonn	DE ELSA	circular	242	52	34	1.499	11 090	0.04	3 GeV 250 pA	50 µm	[50]
2012	Elettra	IT XFEL	circular	52.58	10	20	6.5	7870	0.46	270 pC	(0.33 $\frac{V}{nC\,mm}$X) (0.3 $\frac{V}{nC\,mm}$Y)	[51, 120, 121]
2013	Tsinghua	CN TTX	rectangular	56.66X 54.654Y	15	15	5.653X 5.772Y	8000	—	—	—	[18]

5 Outlook

The purpose of this report is to offer some inspirations for the design of our cavity, whose main challenge is being able to identify the transverse position of each stored ion in the CR. This requires our cavity must be sensitive to the beam intensity down to single ions, and the beam position down to millimeters.

Although most of the CBPM that we have reviewed own the capability of sub-μm position resolution, unfortunately they are all dealing with the bunched beam in a section of linac. Due to a huge amount of particles in one beam bunch, the intensity sensitivity is no longer a issue in their cases. However on the contrary in our case, the stored ions are coasting in the ring during the mass measurement experiment, which makes the ions separately passing through the cavity. As a trade-off, we have to loose the requirement on the position sensitivity in order to gain the sensitivity on the beam intensity.

But still, we do learn some lessons from the history, helping with our exploring direction. Among those four families of CBPM, the choke mode cavity seems to be the least favorite one. It damps almost all the eigenmodes except the desired dipole mode, which is acceptable for the beam acceleration since the energy is fed by the external. Whereas in our case, we need to extract the induced signal from the cavity. If the most energy is damped by the structure, the residual will be buried deeply under the noise. Thus no useful information can be obtained.

The re-entrant cavity is not suitable to our case either, because it is designed for the broadband operation, which is not our original intention. In order to have a high sensitivity, the cavity needs a quite high Q-value, preventing the attenuation of the induced signal. As a direct consequence of high Q-value, the resonant peak is remarkably narrow, recalling that the quality factor is calculated as the ratio of resonant frequency to the width of the resonant peak.

After ruling out the improper ones, we are now facing the choice out of two: rectangular or circular. Based on a whole consideration of manufacturing difficulty and cost efficiency, we prefer the concept of circular cavity as our R&D scheme. According to the actual specifications of the CR, we have already proposed several designs, and simulated their RF properties with a commercial software CST STUDIO SUITE®. Then we have manufactured the first model cavity through an external company, rooted in the most promising design. Meanwhile we have also constructed a computer-controlled testing platform for the cavity bench top measurements. However all of these progresses are beyond the scope of this report, but will be documented elsewhere.

Acknowledgments

This report could not be finished without the strong supports from my colleagues at GSI. In particular, I would like to express my gratitudes to M. S. Sanjari, Yu. A. Litvinov and M. Steck for their invaluable advices and assistances. Moreover, their numerous enthusiasms for the research influence me a lot, which I appreciate very much. This work is funded by the European Commission under contract number PITN-GA-2011-289485.

References

[1] H. H. Gutbrod, I. Augustin *et al.* (editors), "FAIR — baseline technical report: Executive summary", vol. 1. GSI, Darmstadt (2006).

[2] F. Bosch, Yu. A. Litvinov *et al.*, "Nuclear physics with unstable ions at storage rings". *Prog. Part. Nucl. Phys.*, **73** (2013) 84.

[3] P. Forck, P. Kowina *et al.*, "Beam position monitors". *Proceedings of CAS '08: Beam Diagnostics*, Dourdan, France (2008) 187.

[4] A. Wolski, "Theory of electromagnetic fields". *Proceedings of CAS '10: RF for Accelerators*, Ebeltoft, Denmark (2010) 15.

[5] E. Jensen, "Cavity basics". *Proceedings of CAS '10: RF for Accelerators*, Ebeltoft, Denmark (2010) 259.

[6] D. Alesini, "Power coupling". *Proceedings of CAS '10: RF for Accelerators*, Ebeltoft, Denmark (2010) 125.

[7] M. S. Sanjari, "Resonant pickups for non-destructive single-particle detection in heavy-ion storage rings and first experimental results". Thesis, Johann Wolfgang Goethe-Universität Frankfurt am Main (2013).

[8] T. Nakamura, "Development of beam-position monitors with high position resolution". Thesis, University of Tokyo (2008).

[9] P. B. Wilson, "Transient beam loading in electron-positron storage rings". *CERN-ISR-TH-78-23-rev*, CERN, Geneva (1978).

[10] W. Schnell, "Common-mode rejection in resonant microwave position monitors for linear colliders". *CLIC-Note-70*, CERN, Geneva (1988).

[11] R. Bergere, A. Veyssiere *et al.*, "Linac beam position monitor". *Rev. Sci. Instrum.*, **33** (1962) 1441.

[12] R. B. Neal, "An alternate design of a microwave beam position monitor". *TN-63-87*, SLAC, Stanford (1963).

[13] P. Brunet, J. Dobson *et al.*, "Microwave beam position monitors". *TN-64-45*, SLAC, Stanford (1964).

[14] E. V. Farinholt, Z. D. Farkas *et al.*, "Microwave beam position monitors at SLAC". *IEEE Trans. Nucl. Sci.*, **14** (1967) 1127.

[15] Z. Farkas, H. Hogg *et al.*, "Recent developments in microwave beam-position monitors at SLAC". *Proceedings of LINAC '76*, Chalk River, Ontario, Canada (1976) 300.

[16] D. Goldberg, W. Barry *et al.*, "A high-frequency schottky detector for use in the Tevatron". *Proceedings of PAC '87*, Washington, DC, USA (1987) 547.

[17] Y. Inoue, H. Hayano *et al.*, "Development of a high-resolution cavity-beam position monitor". *Phys. Rev. ST Accel. Beams*, **11** (2008) 062801.

[18] J. Su, Y. Du *et al.*, "Design and cold test of a rectangular cavity beam position monitor". *Chinese Phys. C*, **37** (2013) 017002.

[19] J. McKeown, "Beam position monitor using a single cavity". *IEEE Trans. Nucl. Sci.*, **26** (1979) 3423.

[20] K. C. D. Chan, R. T. F. Bird *et al.*, "Experiments with beam position sensors". *IEEE Trans. Nucl. Sci.*, **28** (1981) 2328.

[21] W. Schnell, J. P. H. Sladen *et al.*, "CLIC beam position monitor developments". *Proceedings of HEACC '92*, Hamburg, Germany (1992) 263.

[22] J. P. H. Sladen, I. H. Wilson *et al.*, "CLIC beam position monitor tests". *Proceedings of EPAC '96*, Sitges, Barcelona, Spain (1996) 1609.

[23] H. Euteneuer, H. Herminghaus *et al.*, "Beam monitors at the mainz microtron". *Proceedings of LINAC '92*, Ottawa, Ontario, Canada (1992) 356.

[24] H. Hayano and T. Shintake, "Submicron beam position monitors for japan linear collider". *Proceedings of LINAC '92*, Ottawa, Ontario, Canada (1992) 106.

[25] R. Lorenz and K. Yezza, "Beam position monitors for the TESLA test facility". *TESLA-1993-34*, DESY, Hamburg (1993).

[26] R. Lorenz, M. Sachwitz *et al.*, "First operating experiences of beam position monitors in the TESLA test facility linac". *Proceedings of PAC '97*, Vancouver, Canada (1997) 2137.

[27] V. E. Balakin, A. Bazhan *et al.*, "Beam position monitor with nanometer resolution for linear collider". *Proceedings of EPAC '94*, London, UK (1994) 1539.

[28] V. Balakin, A. Bazhan *et al.*, "Experimental results from a microwave cavity beam position monitor". *Proceedings of PAC '99*, New York, USA (1999) 461.

[29] M. Ross, J. Frisch *et al.*, "Very high resolution RF cavity BPM". *Proceedings of PAC '03*, Portland, Oregon, USA (2003) 2545.

[30] S. Walston, S. Boogert *et al.*, "Performance of a high resolution cavity beam position monitor system". *Nucl. Instrum. Meth. A*, **578** (2007) 1.

[31] R. Ursic, R. Flood *et al.*, "1 nA beam position monitoring system". *Proceedings of PAC '97*, Vancouver, Canada (1997) 2131.

[32] R. Johnson, Z. Li *et al.*, "Cavity BPMs for the NLC". *Proceedings of BIW '02*, Upton, New York, USA (2002) 321.

[33] R. Johnson, Z. Li *et al.*, "An X-band cavity for a high precision beam position monitor". *Proceedings of DIPAC '03*, Mainz, Germany (2003) 196.

[34] A. Liapine, "Beam position monitor for the TESLA energy spectrometer". *Proceedings of EPAC '02*, Paris, France (2002) 1921.

[35] V. Sargsyan, H. Schreiber *et al.*, "Test measurements of a new TESLA cavity beam position monitor at the ELBE linac". *TESLA-2004-14*, DESY, Hamburg (2004).

[36] A. Lyapin, F. Gournaris *et al.*, "A prototype energy spectrometer for the ILC at end station A in SLAC". *Proceedings of PAC '07*, Albuquerque, New Mexico, USA (2007) 4285.

[37] M. Slater, C. Adolphsen *et al.*, "Cavity BPM system tests for the ILC energy spectrometer". *Nucl. Instrum. Meth. A*, **592** (2008) 201.

[38] A. Lyapin, B. Maiheu *et al.*, "Development of the C-band BPM system for ATF2". *Proceedings of PAC '09*, Vancouver, Canada (2009) 4009.

[39] A. Lyapin, B. Maiheu *et al.*, "Development of the S-band BPM system for ATF2". *Proceedings of PAC '09*, Vancouver, Canada (2009) 4003.

[40] Y. I. Kim, R. Ainsworth *et al.*, "Cavity beam position monitor system for the accelerator test facility 2". *Phys. Rev. ST Accel. Beams*, **15** (2012) 042801.

[41] F. Cullinan, S. T. Boogert *et al.*, "A prototype cavity beam position monitor for the CLIC main beam". *Proceedings of IBIC '12*, Tsukuba, Japan (2012) 95.

[42] F. Cullinan, S. T. Boogert *et al.*, "Development of a cavity beam position monitor for CLIC". *Proceedings of IPAC '12*, New Orleans, Louisiana, USA (2012) 915.

[43] A. Lunin, N. Solyak *et al.*, "Design of a submicron resolution cavity BPM for the CLIC main linac". *TD-Note-TD-09-028*, Fermilab, Batavia (2009).

[44] S. Shin and M. Wendt, "Design studies for a high resolution cold cavity beam position monitor". *IEEE Trans. Nucl. Sci.*, **57** (2010) 2159.

[45] M. Wendt, "Cold cavity BPM R&D for the ILC". *Proceedings of CARE-HHH-ABI '06*, Lüneburg, Germany (2006) 39.

[46] A. Lunin, G. Romanov *et al.*, "Design of a submicron cavity BPM for the ILC main linac". *Proceedings of DIPAC '07*, Venice, Italy (2007) 192.

[47] R. Lill, G. Waldschmidt *et al.*, "Linac coherent light source undulator RF BPM system". *Proceedings of FEL '06*, Berlin, Germany (2006) 706.

[48] H. Maesaka, H. Ego *et al.*, "Sub-micron resolution RF cavity beam position monitor system at the SACLA XFEL facility". *Nucl. Instrum. Meth. A*, **696** (2012) 66.

[49] D. Lipka, D. Nölle *et al.*, "Orthogonal coupling in cavity BPM with slots". *Proceedings of DIPAC '09*, Basel, Switzerland (2009) 44.

[50] T. R. Pusch, F. Frommberger *et al.*, "Measuring the intensity and position of a pA electron beam with resonant cavities". *Phys. Rev. ST Accel. Beams*, **15** (2012) 112801.

[51] M. Dal Forno, P. Craievich *et al.*, "A novel electromagnetic design and a new manufacturing process for the cavity BPM (beam position monitor)". *Nucl. Instrum. Meth. A*, **662** (2012) 1.

[52] X. Li and S. Zheng, "Simulation and experiments for the Q_{ext} of a cavity beam position monitor". *Chinese Phys. C*, **34** (2010) 405.

[53] J. Chu, D. Tong *et al.*, "RF measurements of a C-band cavity beam position monitor". *Chinese Phys. C*, **32** (2008) 385.

[54] M. Hansli, R. Jakoby *et al.*, "Current status of the schottky cavity sensor for the CR at FAIR". *Proceedings of IBIC '13*, Oxford, UK (2013) 907.

[55] O. Altenmueller and P. Brunet, "Some RF characteristics of the beam phase reference cavity". *TN-64-51*, SLAC, Stanford (1964).

[56] R. Bossart, "Microwave beam position monitor using a re-entrant coaxial cavity". *CERN-PS-91-59-LP*, CERN, Geneva (1992).

[57] R. Bossart, "High precision beam position monitor using a re-entrant coaxial cavity". *Proceedings of LINAC '94*, Tsukuba, Japan (1994) 851.

[58] C. Magne, M. Juillard *et al.*, "High resolution BPM for future colliders". *Proceedings of LINAC '98*, Chicago, Illinois, USA (1998) 323.

[59] C. Magne and M. Wendt, "Beam position monitors for the TESLA accelerator complex". *TESLA-2000-41*, DESY, Hamburg (2000).

[60] C. Simon, M. Luong *et al.*, "Performance of a reentrant cavity beam position monitor". *Phys. Rev. ST Accel. Beams*, **11** (2008) 082802.

[61] R. Lorenz, S. Sabah *et al.*, "Cavity-type beam position monitors for the SASE FEL at the TESLA test facility". *TESLA-FEL-2003-03*, DESY, Hamburg (2003).

[62] Q. Luo, B. Sun *et al.*, "Cold test of S-band re-entrant cavity BPM for HLS". *Proceedings of IPAC '10*, Kyoto, Japan (2010) 1032.

[63] T. Shintake, "The choke mode cavity". *KEK-Preprint-92-51*, KEK, Tsukuba (1992).

[64] S. C. Hartman, T. Shintake *et al.*, "Nanometer resolution BPM using damped slot resonator". *Proceedings of PAC '95*, Dallas, Texas, USA (1995) 2655.

[65] T. Shintake, "Development of nanometer resolution RF-BPMs". *Proceedings of HEACC '98*, Dubna, Russia (1998) 341.

[66] T. Slaton, G. Mazaheri *et al.*, "Development of nanometer resolution C-band radio frequency beam position monitors in the final focus test beam". *Proceedings of LINAC '98*, Chicago, Illinois, USA (1998) 911.

[67] M. J. Lee, "The effect of rotation of a TM_{120} cavity on the amplitude and phase of the beam induced signal". *TN-64-66*, SLAC, Stanford (1964).

[68] J. P. H. Sladen and W. Wuensch, "Loss of precision in resonant beam position monitors due to finite Q". *Proceedings of PAC '93*, Washington, DC, USA (1993) 2346.

[69] J. P. H. Sladen, "Receiver for CLIC resonant microwave position monitors". *CLIC-Note-86*, CERN, Geneva (1989).

[70] J. P. H. Sladen, I. H. Wilson *et al.*, "Measurement of the precision of a CLIC beam position monitor". *CLIC-Note-189*, CERN, Geneva (1993).

[71] J. P. H. Sladen and W. Wuensch, "The effect of finite Q on the precision of resonant beam position monitors". *CLIC-Note-185*, CERN, Geneva (1993).

[72] J. Sladen, "Signal processing for the CLIC beam position monitor". *Proceedings of EPAC '90*, Nice, France (1990) 735.

[73] R. Lorenz, "RF beam position monitors for the TESLA test facility". *Proceedings of PAC '93*, Washington, DC, USA (1993) 2325.

[74] R. Lorenz and K. Yezza, "Test results on a beam position monitor prototype for the TTF". *Proceedings of EPAC '94*, London, UK (1994) 1536.

[75] R. Lorenz, S. Sabah *et al.*, "Electronics for the TTFL cavity-type beam position monitor". *Proceedings of EPAC '98*, Stockholm, Sweden (1998) 1553.

[76] R. Lorenz, "Beam position monitors in the TESLA test facility linac". *Proceedings of PAC '95*, Dallas, Texas, USA (1995) 2631.

[77] R. Lorenz, M. Sachwitz *et al.*, "Measurement of the beam position in the TESLA test facility linac". *Proceedings of LINAC '96*, Geneva, Switzerland (1996) 527.

[78] H. Dong, A. Freyberger *et al.*, "Digital beam position monitor for the HAPPEX experiment". *Proceedings of PAC '05*, Knoxville, Tennessee, USA (2005) 3841.

[79] S. Smith, "Cavity beam position monitors for the next linear collider" (2002).

[80] Z. Li, R. Johnson *et al.*, "Cavity BPM with dipole-mode-selective coupler". *Proceedings of PAC '03*, Portland, Oregon, USA (2003).

[81] Z. Li, "S-band cavity BPM for ILC" (2005).

[82] A. Liapine, "Cavity beam position monitor for the TESLA energy spectrometer". *Proceedings of DIPAC '03*, Mainz, Germany (2003) 184.

[83] A. Liapine and H. Henke, "High precision cavity beam position monitor". *Proceedings of EPAC '04*, Lucerne, Switzerland (2004) 2535.

[84] V. Sargsyan, "Cross-talk problem in pill-box cavity". *TESLA-2003-01*, DESY, Hamburg (2003).

[85] M. Ross, J. Frisch *et al.*, "RF cavity BPM's as beam angle and beam correlation monitors". *Proceedings of PAC '03*, Portland, Oregon, USA (2003) 2548.

[86] V. Vogel, H. Hayano *et al.*, "Performance of a nanometer resolution beam position monitor system". *UCRL-CONF-216283*, LLNL, Livermore (2005).

[87] S. Walston, C. Chung *et al.*, "Resolution of a high performance cavity beam position monitor system". *Proceedings of PAC '07*, Albuquerque, New Mexico, USA (2007) 4090.

[88] S. Walston, S. Boogert *et al.*, "A metrology system for a high resolution cavity beam position monitor system". *Nucl. Instrum. Meth. A*, **728** (2013) 53.

[89] P. Krejcik, Z. Li *et al.*, "Cavity beam position monitors in the LCLS" (2006).

[90] R. Lill, W. Norum *et al.*, "Design and performance of the LCLS cavity BPM system". *Proceedings of PAC '07*, Albuquerque, New Mexico, USA (2007) 4366.

[91] G. Waldschmidt, R. Lill *et al.*, "Electromagnetic design of the RF cavity beam position monitor for the LCLS". *Proceedings of PAC '07*, Albuquerque, New Mexico, USA (2007) 1153.

[92] S. Smith, S. Hoobler *et al.*, "LCLS cavity beam position monitor". *Proceedings of DIPAC '09*, Basel, Switzerland (2009) 285.

[93] A. Lyapin, B. Maiheu *et al.*, "A prototype S-band BPM system for the ILC energy spectrometer". *EUROTeV-Report-2008-072*, UCL, London (2009).

[94] S. H. Shin, E. S. Kim *et al.*, "The design study for low-Q IP-BPM". *Proceedings of PAC '07*, Albuquerque, New Mexico, USA (2007) 4120.

[95] A. Heo, E. S. Kim *et al.*, "Nanometer resolution beam position monitor for the ATF2 interaction point region". *Proceedings of PAC '09*, Vancouver, Canada (2009) 3603.

[96] S. Jang, E. S. Kim *et al.*, "Development of a cavity-type beam position monitors with high resolution for ATF2". *Proceedings of IPAC '13*, Shanghai, China (2013) 604.

[97] A. Lyapin and S. T. Boogert, "A proposal of a single coupler cavity beam position monitor". *Proceedings of PAC '09*, Vancouver, Canada (2009) 4000.

[98] C. Simon, S. Chel *et al.*, "High resolution BPM for linear colliders". *Proceedings of BIW '06*, Batavia, Illinois, USA (2006) 488.

[99] C. Simon, S. Chel *et al.*, "Beam position monitors using a re-entrant cavity". *Proceedings of DIPAC '07*, Venice, Italy (2007) 93.

[100] C. Simon, S. Chel *et al.*, "High resolution BPM for linear colliders". *Proceedings of EPAC '06*, Edinburgh, Scotland (2006) 1004.

[101] C. Simon, O. Napoly *et al.*, "Status of the re-entrant cavity beam position monitor for the european XFEL project". *Proceedings of BIW '10*, Santa Fe, New Mexico, USA (2010) 210.

[102] B. Wang, Y. Leng *et al.*, "Study of the signal processing system for cavity beam position monitor". *Proceedings of IPAC '12*, New Orleans, Louisiana, USA (2012) 855.

[103] A. Lyapin, R. Ainsworth *et al.*, "Cavity BPM system for ATF2". *Proceedings of DIPAC '11*, Hamburg, Germany (2011) 23.

[104] S. T. Boogert, R. Ainsworth *et al.*, "Cavity beam position monitor system for ATF2". *Proceedings of IPAC '10*, Kyoto, Japan (2010) 1140.

[105] S. T. Boogert, G. Boorman *et al.*, "Cavity beam position monitor system for ATF2". *Proceedings of IPAC '11*, San Sebastián, Spain (2011) 1410.

[106] F. Cullinan, S. T. Boogert *et al.*, "Calibration errors in the cavity beam position monitor system at the ATF2". *Proceedings of IPAC '11*, San Sebastián, Spain (2011) 1051.

[107] S. Shin, E. S. Kim *et al.*, "Design of a low-Q S-band cavity beam position monitor". *J. Korean Phys. Soc.*, **52** (2008) 992.

[108] A. Heo, E. S. Kim *et al.*, "Development of an S-band cavity beam position monitor for ATF2". *J. Inst.*, **8** (2013) P04011.

[109] D. Lipka, "Cavity BPM designs, related electronics and measured performances". *Proceedings of DIPAC '09*, Basel, Switzerland (2009) 280.

[110] H. Schmickler, L. Soby *et al.*, "Submicron multi-bunch BPM for CLIC". *Proceedings of IPAC '10*, Kyoto, Japan (2010) 1185.

[111] A. Lunin, "High resolution RF cavity BPM design for linear collider" (2012).

[112] Q. Luo, B. Sun *et al.*, "Design of cavity beam monitor at HLS". *Proceedings of IPAC '11*, San Sebastián, Spain (2011) 1278.

[113] Q. Luo, B. Sun *et al.*, "Design of racetrack cavity beam position monitor". *Proceedings of PAC '09*, Vancouver, Canada (2009) 4084.

[114] Q. Luo, B. Sun *et al.*, "Design and cold test of re-entrant cavity BPM for HLS". *Proceedings of PAC '11*, New York, USA (2011) 420.

[115] M. Hansli, A. Angelovski *et al.*, "Coupling methods for the highly sensitive cavity sensor for longitudinal and transverse schottky measurements". *Proceedings of BIW '12*, Newport News, Virginia, USA (2012) 149.

[116] M. Hansli, A. Angelovski *et al.*, "Investigations on high sensitive sensor cavity for longitudinal and transversal schottky for the CR at FAIR". *Proceedings of IPAC '11*, San Sebastián, Spain (2011) 1180.

[117] M. Hansli, A. Penirschke *et al.*, "Conceptual design of a high sensitive versatile schottky sensor for the collector ring at FAIR". *Proceedings of DIPAC '11*, Hamburg, Germany (2011) 470.

[118] H. Maesaka, Y. Otake *et al.*, "Beam position monitor at the SCSS prototype accelerator". *Proceedings of APAC '07*, Indore, India (2007) 387.

[119] H. Maesaka, S. Inoue *et al.*, "Development of the RF cavity BPM of XFEL/SPring-8". *Proceedings of DIPAC '09*, Basel, Switzerland (2009) 56.

[120] P. Craievich, D. Castronovo *et al.*, "Design of the cavity BPM for FERMI@Elettra". *Proceedings of FEL '06*, Berlin, Germany (2006) 613.

[121] P. Craievich, C. Bontoiu *et al.*, "Design of the cavity BPM system for FERMI@Elettra". *Proceedings of DIPAC '07*, Venice, Italy (2007) 165.